

Quantifying the impact of urban trees on land surface temperature in global cities

Tingting He^{a,1}, Yihua Hu^{b,1}, Andong Guo^{a,*}, Yuwei Chen^{c,d}, Jun Yang^e, Mengmeng Li^a, Maoxin Zhang^a

^a Department of Land Management, Zhejiang University, Hangzhou 310058, China

^b State Key Laboratory of Pulsed Power Laser Technology, Hefei 230000, China

^c Advanced Laser Technology Laboratory of Anhui Province, Hefei 230000, China

^d Jinhua Institute of Zhejiang University, Jinhua 321004, China

^e Jangho Architecture College, Northeastern University, Shenyang 110169, China



ARTICLE INFO

Keywords:

Tree canopy height
Land surface temperature
Cooling effect
Building form
Random forests

ABSTRACT

Urban trees are not only a core component of natural infrastructure but also an effective way to mitigate urban heat with nature-based solutions. Comprehensively revealing the cooling effects of trees and their drivers is valuable for enhancing urban climate resilience and promoting sustainable development. While existing studies have investigated the cooling effects of two-dimensional characteristics of trees, there has been limited consideration of the effects of vertical structure, especially in various climatic zones across the globe. In this study, we employed the Google Earth Engine cloud platform and the random forest algorithm to comprehensively assess the impact of three-dimensional (3D) characteristics of trees on land surface temperature across 596 cities worldwide. Results suggest that LST is generally lower in tree-covered areas than their surrounding built-up land, especially in the summer, with an average decrease of about 2.13 °C. We also found a significant negative correlation between tree canopy height and LST (~ -0.83). Specifically, the mean LST decreases by about 0.16 °C for every 1m increase in tree height. Globally, the average cooling intensity of trees is 1.86 °C, and is about 1.06 °C higher in summer than in winter. It is worth noting that during winter, the cooling effect of trees is more pronounced closer to the equator. In addition, the 3D characteristics of trees contribute more significantly to cooling intensity compared to their surrounding environmental factors. This study not only fills a global knowledge gap regarding the impact of 3D features of trees on LST, but also provides valuable insights into urban planning and management in response to climate change.

1. Introduction

In recent decades, the world has experienced rapid urbanization. According to United Nations projections, nearly 70 percent of global population will reside in urban areas by 2050 (Nations, 2018). However, rapid urbanization has not only changed land cover, but also exacerbated the impact of human activities on the surface energy balance, seriously affecting ecosystems and urban climates (Grimm et al., 2008; Han et al., 2015). Particularly, the Urban Heat Island (UHI) effect has emerged as a global concern. This phenomenon typically manifests as higher temperatures within cities compared to their surrounding rural areas (Howard, 1818; Voogt and Oke, 2003). Numerous studies have

demonstrated that UHI not only exacerbates air pollution, but also threatens the health of local residents (Patz et al., 2005; Yin et al., 2023). Land Surface Temperature (LST), a key indicator for measuring surface UHI, has received widespread attention because its spatiotemporal characteristics and driving forces can be revealed through remote sensing techniques, thus offering strong supports for urban heat mitigation.

Tree planting is considered a nature-based solution and one of the preferred strategies for cooling cities (Bartesaghi-Koc et al., 2020; Jungman et al., 2023). Numerous studies have confirmed that urban trees reduce air temperature primarily through altering shade and evapotranspiration. Tree canopies provide natural shade, effectively

* Corresponding author.

E-mail address: guandong@zju.edu.cn (A. Guo).

¹ Equal contribution.

blocking solar radiation and creating a cooler environment in their surrounding area (Rahman et al., 2020; Yu et al., 2020a). Studies have shown that surface temperatures beneath a shaded canopy are significantly lower than in areas exposed to sunlight (Speak et al., 2020), LST was negatively correlated with Leaf Area Index (LAI), with cooling ranging from 13.8 to 22.8 °C (Napoli et al., 2016). Moreover, trees undergo evapotranspiration through the stomata on their leaves, converting water into water vapor, thereby reducing leaf surface temperature and canopy temperature (Leuzinger et al., 2010). Wang et al., (2019a) noted that cooling efficiency is mainly influenced by vegetation transpiration, with their cooling efficiency increasing by 1.34 °C per fractional tree cover (FTC) during heat waves. It is worth noting that tree transpiration is highly dependent on a wide range of factors such as tree species, health status, seasonal variation, and location (Winbourne et al., 2020).

To date, scholars have used numerous methods to assess the cooling effect of trees, including fixed and mobile measurements, numerical modeling (CFD, ENVI-Met), and remote sensing techniques (Park et al., 2012; Parison et al., 2023). Although both fixed and mobile measurements and numerical modeling provide highly accurate data, these methods are costly and limited in spatial scale. In contrast, remote sensing techniques, which provide comprehensive information on the urban thermal environment, and are characterized by flexibility in spatial and temporal resolution, have been widely used to assess cooling effect (Wang et al., 2019b; Yang et al., 2022). To deeply understand the tree-cooling effect as well as its geographical differences, scholars have carried out systematic analyses based on MODIS, Landsat, and other data by constructing indicators such as cooling efficiency, cooling intensity and the extend of cooling, which provide an important tool for elucidating the tree-cooling effect (Zhou et al., 2017; Zhao et al., 2023; Chang et al., 2023).

Despite numerous scholars on the cooling effects of trees, two issues remain to be further explored. First, most studies have focused on the two-dimensional characteristics of trees, such as vegetation cover and canopy shape, and knowledge of the vertical height of trees in different climatic zones on a global scale is still limited (Du et al., 2016; Wang et al., 2023a). It has been shown that the cooling effect of trees is closely related to their vertical height, but due to limited data availability, as well as methodological and technological limitations, most of the existing studies are confined to a few cities and further lack quantitative analyses regarding the effect of trees on LST on a global scale (Gage and

Cooper, 2017; Chen et al., 2020). Second, there is a lack of clear knowledge about the non-linear effects of the 3D characteristics of trees on cooling intensity. When revealing the drivers of tree cooling intensity, scholars mostly focus on the tree's inherent characteristics, especially its scale and landscape features. However, factors such as green spaces, water bodies and the buildings that surround the trees also influence LST (Guo et al., 2020a; Guo et al., 2022), thus indirectly altering their cooling effect (Zhang et al., 2022). This suggests that the cooling effect is not only closely related to their inherent characteristics but also to their surroundings, which play an important role (Liao et al., 2023). Notably, linear regression analyses have failed to accurately reveal the complex associations between such factors and tree-cooling intensity.

In this study, we aim to explore the cooling effect and its associated drivers in terms of 3D features of urban trees at a global scale. Specifically, we focused on answering the following research questions: (1) How much difference does LST between tree cover and surrounding built-up land? (2) How does tree canopy height affect LST? (3) What factors are important drivers of tree-cooling intensity?

2. Materials and methods

2.1. Study area

We selected 596 urban areas around the world (Fig. 1). These cities were obtained from the global dataset of artificial impervious areas dataset (Li et al., 2020), with the specific criterion necessitating an area larger than 50 km². Although more than 1,000 potential cities were initially screened, we ultimately excluded some cities due to an insufficient number of trees in the sample (Yang et al., 2021; Chen et al., 2022). These selected cities are located in 88 countries or regions around the world, with 113 and 171 cities in China and the United States, respectively. To investigate the effect of urban climate on tree cooling, we used the Köppen climate classification for global cities (Peel et al., 2007). The classification is based on long-term global precipitation and temperature observations, as well as natural vegetation distribution, which in turn has led to the generation of a gridded 0.1° resolution global climate maps. The classification consists of 5 major climate zones (Tropical, Arid, Temperate, Cold, and Polar) and 30 subclimate-type zones. In this study, these 596 selected cities are concentrated in 16 climate zones, with the highest number of cities in the Cfa (160) and Dfa

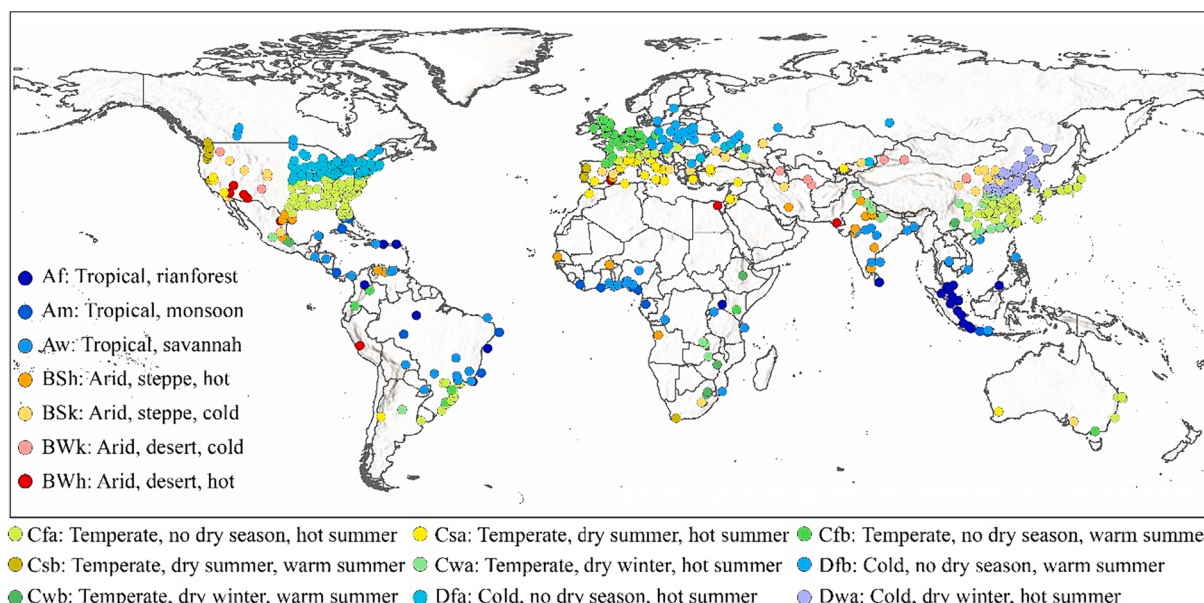


Fig. 1. The location of study area.

(73) climatic zones.

2.2. Data selection and processing

The datasets mainly consist of Landsat-8, land cover, tree canopy height, building footprint, and Digital Elevation Model (DEM). Landsat-8, land cover, and tree canopy height data are used to quantify the cooling effect of trees, whereas the building footprint and DEM are considered as significant impact factors.

We use Landsat-8 data directly through the GEE platform, which has been resampled to a 30 m spatial resolution by the USGS. To ensure the accuracy of LST inversion, we selected the lowest cloud scenario with less than 15 % cloud coverage. Moreover, since the seasons are opposite in the northern and southern hemispheres, we selected remote sensing images for summer (June-August) and winter (December-February) in the northern hemisphere and conversely in the southern hemisphere (Yang et al., 2022). When the city did not have applicable 2020 Landsat-8 imagery, we used the 2019 and 2021 data to substitute.

Land cover and canopy height were obtained from the European Space Agency WorldCover products and Lang et al. (2022), respectively, both with a spatial resolution of 10 m. WorldCover is the world's first 10 m resolution land cover dataset produced by VITO Remote Sensing in collaboration with many other research organizations through the fusion of Sentinel-1 and Sentinel-2 data, including 11 categories such as tree cover, shrubland, and grassland (Zanaga et al., 2021). The dataset has been validated with an overall accuracy of approximately 74.4 %. Tree canopy height, on the other hand, was extracted by fusing GEDI and Sentinel-2 data and using the convolutional neural network algorithm.

Building footprint and DEM data are factors influencing the trees cooling intensity. The building footprint data, on the one hand, is derived from Microsoft, which was generated using a convolutional neural network semantic segmentation algorithm based on Bing Maps images for the period from 2014 to 2021 (Carlson et al., 2022). However, since this dataset does not cover the Chinese region, we additionally supplemented it with the Chinese multi-year high-resolution building roof area dataset published by Liu et al. (2023). The DEM, on the other hand, is derived from the ASTER product in the GEE cloud platform with a spatial resolution of 30 m.

2.3. Retrieval of land surface temperature

The GEE cloud platform has significant advantages in calculating and analyzing LST on a global scale. In this study, we employ Landsat 8 remote sensing images with the help of the GEE cloud platform and use the Statistical Mono-Window (SMW) algorithm to invert the LST spatial patterns of 596 urban areas (Ermida et al., 2020). Briefly, the SMW algorithm is mainly based on the empirical relationship between the top of the atmosphere (TOA) brightness temperature, the surface emissivity of the corresponding bands, and the surface temperature. The specific calculations are as follows:

$$LST = A_i \frac{T_b}{\epsilon} + B_i \frac{1}{\epsilon} + C_i \quad (1)$$

where T_b represents the TOA bright temperature in the thermal infrared (TIR) channel, and ϵ represents its surface albedo. The parameters A_i , B_i and C_i in the algorithm are determined by performing linear regression analysis for 10 different atmospheric column water vapor classes. These classes have a water vapor range of 0–6 cm, with an interval of 0.6 cm between each class.

2.4. Urban tree-cooling effect

The cooling effect of trees is usually reflected in its difference from the LST of the surrounding environment. Currently, scholars have used more indicators to describe the cooling effect, such as cooling intensity,

cooling extend, cooling efficiency (Wang et al., 2020; Cheng et al., 2022). To more precisely quantify the cooling effect of trees, we assessed the following three aspects: (1) LST difference: we compared the difference in LST between tree cover and its surrounding built-up land by setting a 600 m buffer zone of tree samples (Fig. 2a). This distance was determined based on the establishment of 20 buffers with a step length of 30 m when calculating the cooling effect of green spaces (Peng et al., 2021). (2) Relationship between tree canopy height and LST: we further explored the correlation between tree canopy height and LST (Fig. 2b), especially the magnitude of LST reduction caused by each 1 m increase in canopy height. It should be noted that when analyzing the relationship between canopy height and LST, since the tree cover and LST pixels are 10 m and 30 m, respectively, considering this limitation, we only selected LST pixels with 100 % tree cover for analysis. (3) Cooling intensity: in general, the further away from the trees, the more likely the LST will increase (Fig. 2c). Therefore, numerous scholars have defined the difference between LST at the first turning point and tree samples as the cooling intensity (Yu et al., 2018a; Peng et al., 2021). Specifically, we constructed the LST-distance cubic polynomial by setting the distance from the tree as the independent variable and each buffer LST as the dependent variable. Fig. 2c shows that the LST increase rate continues to decrease with increasing distance from the trees until it reaches zero, which is referred to as the first turning point.

Measuring the cooling intensity of trees is primarily a matter of sample selection (Fig. 2d). To accurately assess the cooling intensity of trees, we followed three main rules: (1) only select tree samples with an area of more than 1 ha to avoid errors in image classification; (2) exclude samples located in a 1-km buffer zone at the city boundary to eliminate suburban interference; (3) exclude samples within 300 m of a water body to avoid interference from its strong cooling effect (Tan et al., 2021). Given these guidelines, we selected a total of more than 20,000 samples and constructed 20 buffers with a step size of 30 m for each sample to identify the cooling intensity.

2.5. Variables influencing the cooling intensity of tree

Tree cooling intensity is influenced by a combination of numerous factors, such as tree area and canopy height, elevation, and the surrounding environment (Masoudi et al., 2019; Hu et al., 2023). To reveal the drivers of cooling intensity, we selected a total of 11 factors to evaluate in combination with the 3D features of the trees and the surrounding environment (Table 1). For the metrics associated with 3D tree characteristics, we selected area, Normalized Difference Vegetation Index (NDVI), DEM and canopy height. A key benefit to using NDVI is that it not only assesses the vegetation cover but also reveals the vegetation growth, which is closely related to the transpiration and shading of vegetation (Guo et al., 2020b). A DEM affects LST by influencing factors such as climate, soil, and light, etc. For canopy height, we counted the maximum, minimum, and standard deviation of trees. In addition to the tree's intrinsic properties, its cooling intensity is inevitably affected by the surrounding environment, especially the neighboring buildings or green spaces which may exert either a facilitating or inhibiting effect (Zhang et al., 2022; Huang and Wang, 2019). Therefore, we included the building density, building area, green space area, built-up land area, and NDVI of the surrounding area around the trees as drivers. It should be emphasized that the green space defined here is the total area of surrounding trees, shrubs and grass. In addition, the extent of the tree perimeter was set to 300 m, which serves as a reference to the subsequent results.

2.6. Statistical analysis

We used a random forest algorithm to reveal the non-linear association between tree-cooling intensity and the multiple influencing factors to make up for the inadequacy of traditional linear regression in resolving such complex relationships. A random forest model, first

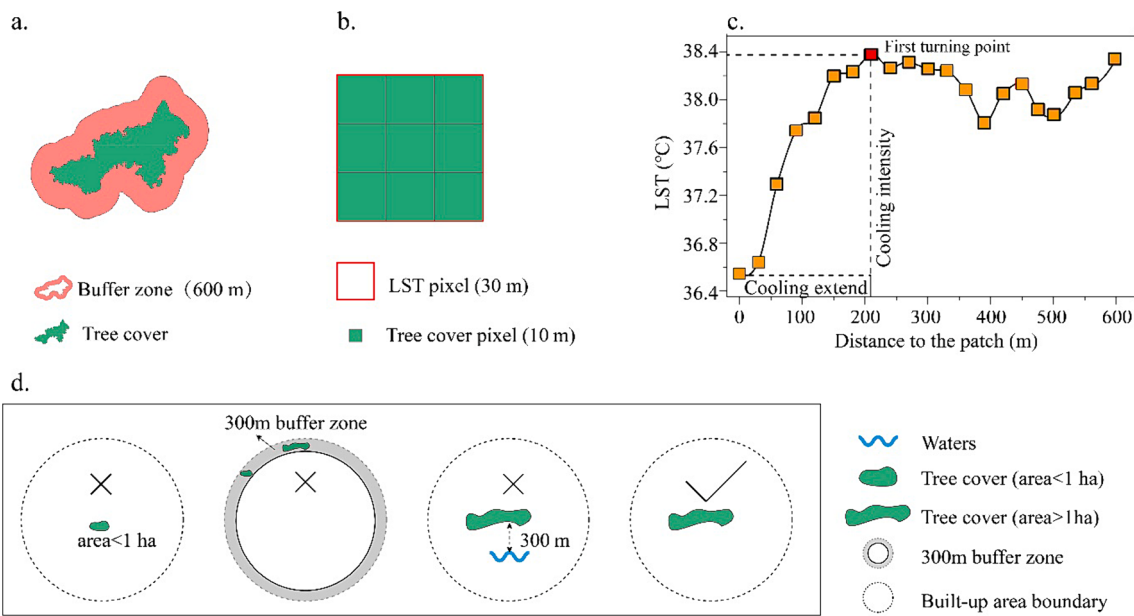


Fig. 2. Cooling effects of trees (a. LST difference between tree cover and surrounding built-up land; b. Tree canopy height and LST correlation; c. Tree cooling intensity; d. Selection rules for tree samples).

Table 1
Description of each influence factor.

Dimension	Category	Factor	Description	Unit
3D features	Size	Tree_Area	Area of selected tree samples	ha
	Spectral index	Tree_NDVI	Seasonal mean NDVI of tree samples (winter and summer)	–
	Elevation	Tree_DEM	Mean DEM value for tree samples	m
	Tree canopy height	TCH_Mean	Mean canopy height of selected tree samples	m
		TCH_Max	Maximum canopy height of selected tree samples	m
		TCH_SD	Standard deviation canopy height in selected tree samples	m
Surrounding environment	Building form	Building density (S_BD)	Building density surrounding the selected tree samples	%
		Building area (S_BA)	Total building area surrounding the selected tree samples	m ²
	Land cover type	Surrounding green space area (S_GSA)	Total green space area surrounding the selected tree samples	m ²
		Surrounding built-up area (S_Built-up)	Total built-up area surrounding the selected tree samples	m ²
Spectral index	S_NDVI	Mean NDVI surrounding the selected tree samples	–	

proposed by Breiman (2001), is a machine learning algorithm based on the idea of bagging, which is widely used in problems such as classification, regression and feature selection. The algorithm aims to optimize the accuracy and robustness of the model by integrating the predictions from multiple decision trees. Specifically, each decision tree is trained on a random subset of the original data, which enhances the model's ability to capture data complexity and diversity. Crucially, in constructing each decision tree, the algorithm randomly selects a subset from all possible features at each decision node and searches for the optimal splitting rule, effectively reducing the risk of overfitting.

One of the major strengths of a random forest model is its ability to effectively reveal complex non-linear relationships between independent and dependent variables (Gao et al., 2023). This is mainly due to its tree-based structure, which is capable of recursively partitioning the data and capturing the nonlinearities and interaction effects therein. In addition, the algorithm provides a way to quantify the importance of features, which helps to gain insight into which variables play a decidedly important role in the prediction process, even if these relationships are characterized by nonlinearity. Overall, a random forest model is a highly flexible and powerful machine learning algorithm particularly suitable for dealing with complex, high-dimensional and non-linear data problems, and has been widely used in a variety of disciplines such as ecology and environmental science (Guo et al., 2023; Peng et al., 2023).

3. Results

3.1. LST differences in tree-covered and surrounding built-up land

Globally, we observe that LST is generally lower in the tree-covered area than in the surrounding built-up land, and this trend is particularly pronounced in the summer, with an average LST decrease of ~ 2.13 °C (Fig. 3a). At this time, several cities in China and the United States performed particularly well, where the maximum LST difference was as high as 4 °C. However, the LST difference narrows in winter, averaging ~ 0.45 °C. Interestingly, we also find that 110 cities show the opposite characteristics in winter, with an average LST higher by about 0.38 °C, and most of these cities are located in the Dwa zone.

In winter, the cooling effect of trees is more pronounced near the equator (Fig. 3b). For example, cities located within the tropics have a lower LST difference (~ 1.30 °C) than other regions. In addition, there

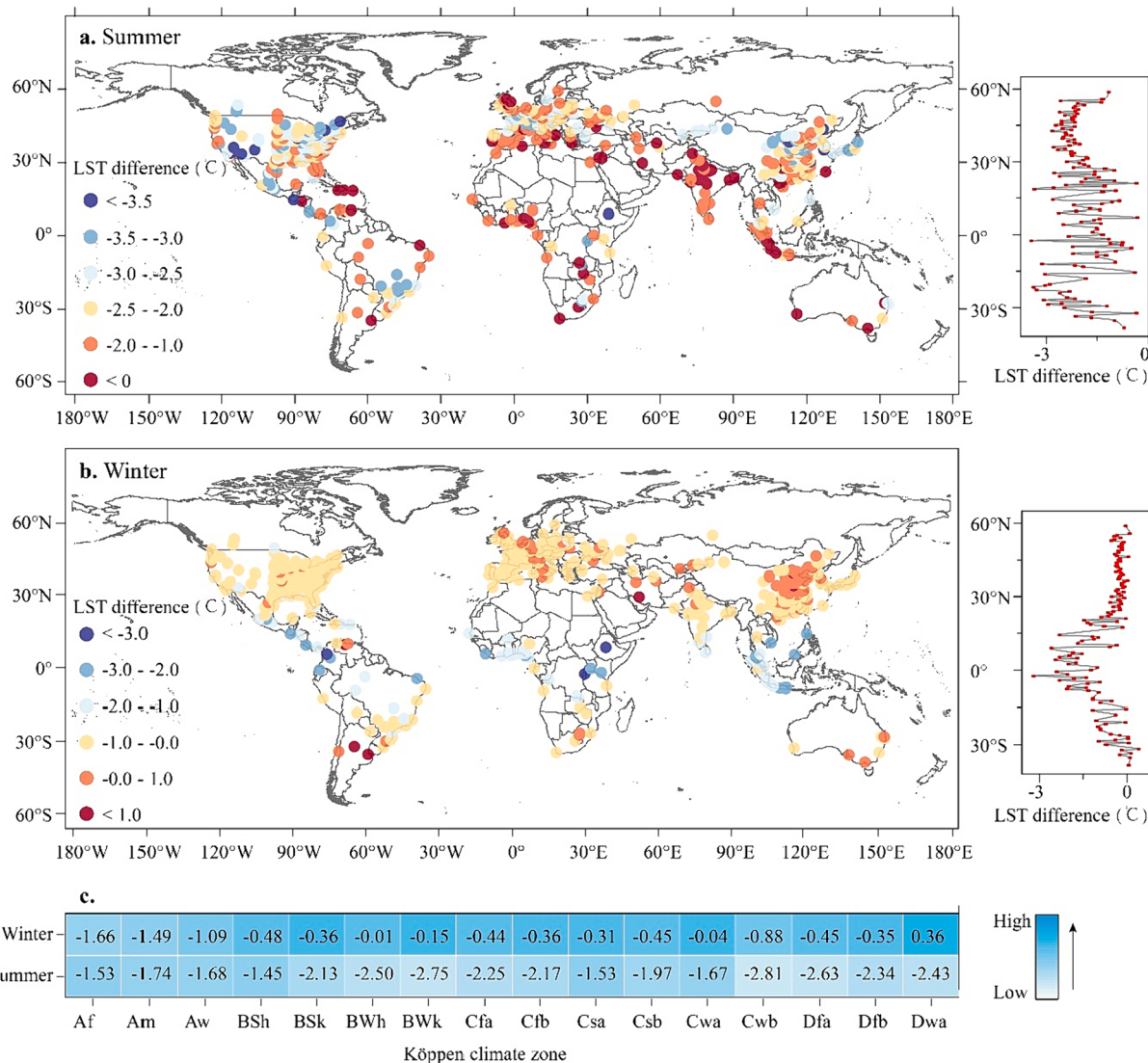


Fig. 3. LST differences in tree cover and surrounding building sites (a and b represent summer and winter LST differences, respectively; c represents each climate zone).

were significant seasonal differences in cooling effects (Fig. 3c). In summer, trees in all climatic zones generally showed a cooling effect, especially in the BWk zone (-2.75°C) and Cwb zone (-2.81°C). However, in winter, the trees in the Dwa zone were approximately 0.36°C warmer than the surrounding built-up land. Overall, the LST difference between Af and Am zones is similar in winter and summer, about 1.60°C and 1.61°C , respectively, and many of these cities are situated in coastal regions close to the equator.

3.2. Tree canopy height and LST correlation

A notable negative correlation was observed between tree canopy height and LST. Specifically, the mean value of the correlation was -0.83 in all climate zones (Fig. 4a), and the correlation was more prominent in Cwb and Csa, which were -0.91 and -0.90 , respectively, implying that LST decreased significantly with the increase of tree height. In addition, nearly 64 % of the cities had the absolute values of their correlation higher than 0.80 . Importantly, despite the generally strong correlation between canopy height and LST, there are still areas with lower correlations, which may be attributed to the potential effects of tree sample selection, elevation, and surroundings on LST.

We also found that with every 1 m rise in tree height, the average LST

decreased by about 0.16°C across climate zones. In particular, the LST decrease was significantly higher in summer (0.21°C) than in winter (0.1°C), with a difference of about 0.11°C (Fig. 4b). In Am and Aw zones, the canopy height and LST declines were even more significant, averaging 0.20°C . Notably, trees in the Aw zone consistently experienced higher cooling in winter and summer, with a seasonal difference of only 0.04°C .

3.3. Spatial patterns of tree cooling intensity

Globally, tree cooling intensity averaged about 1.86°C (Fig. 5a). Seasonally, the cooling intensity is more pronounced in summer, with a value of 2.66°C , compared to 1.06°C in winter. Interestingly, we find that tree cooling intensity is more pronounced in cities closer to the equator in winter, where the cities exceeding 2.0°C are mostly distributed (Fig. 5b). In addition, cities distributed poleward of the Tropic of Cancer experience relatively weaker tree-cooling intensity, with values closer to 0.5°C .

In terms of seasonal differences, tree cooling intensity was significantly stronger in summer than in winter in BWk, Dfa, and Dwa zones, which were 2.60°C , 2.41°C , and 2.25°C higher, respectively (Fig. 5c). However, the difference in cooling intensity in the Af, Am, Aw and BSh

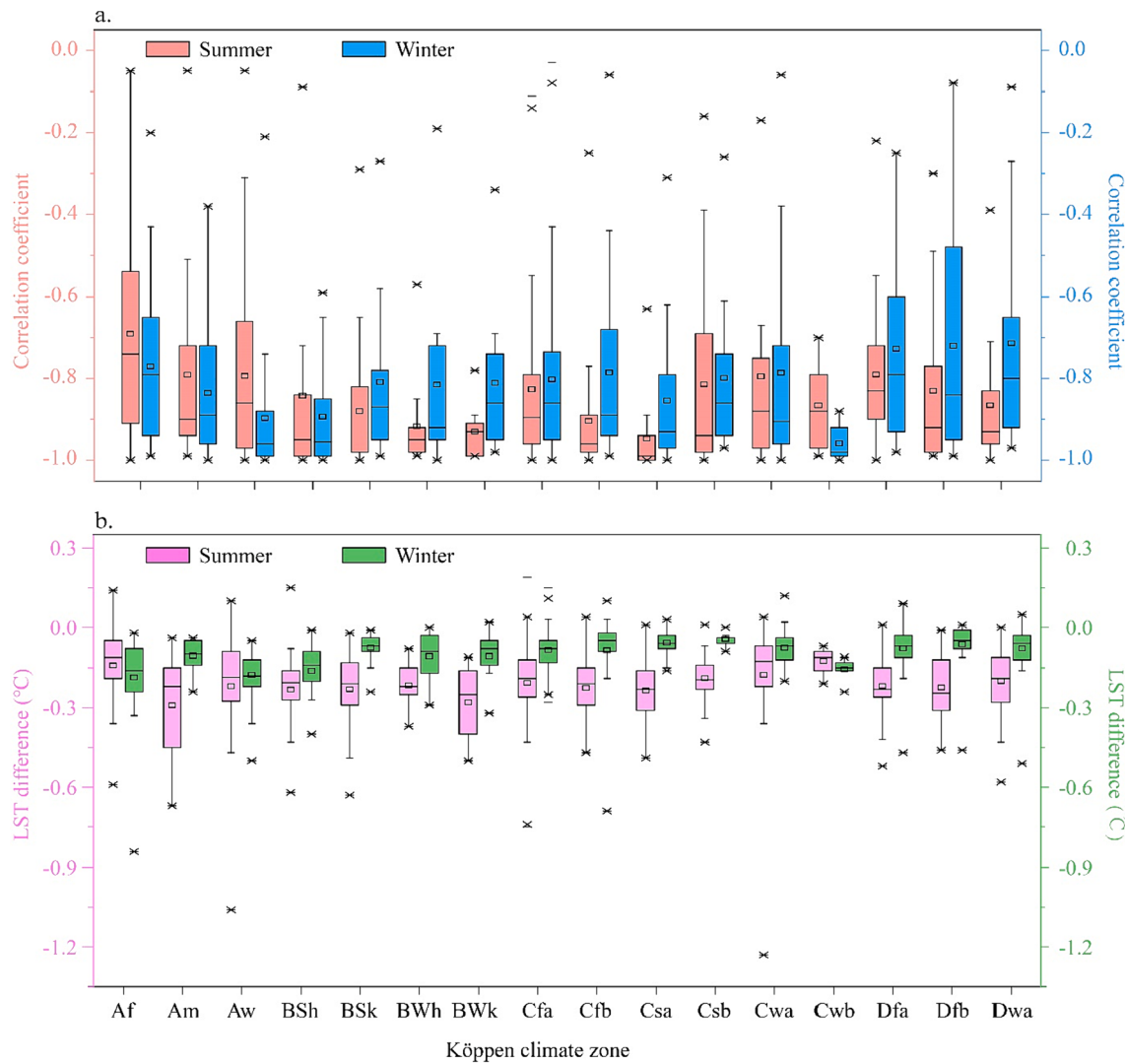


Fig. 4. Relationship between tree canopy height and LST (a represents correlation; b represents decrease in LST per 1 m increase in canopy height).

zones was relatively small, about 0.63°C .

3.4. Drivers of tree-cooling intensity

We found that the random forest method can well explain the driving forces in each climate zone ($R^2 = \sim 0.54$). Fig. 6 shows that the factors affecting the cooling intensity vary significantly across climate zones. In summer, Tree_Area, Tree_NDVI, Tree_DEM and TH_Mean were identified as important factors, especially Tree_NDVI (0.15) and Tree_DEM (0.13). Compared to summer, the importance of the factors was adjusted in winter, with TH_SD and TH_Mean becoming important factors in addition to Tree_NDVI and Tree_DEM. Globally, the surrounding building patterns also have different neglected effects. Specifically, the importance of S_BA importance is 0.09 and 0.13 in summer and winter, respectively. In summary, Tree_Area, Tree_NDVI, Tree_DEM, and TH_Mean are important influences factors in all climate zones and seasons.

To further reveal the non-linear relationship between the driving factors and trees' cooling intensity, we plotted the marginal effect curves of the four key factors, namely Tree_Area, Tree_NDVI, Tree_DEM and TH_Mean (Fig. 7). The marginal effect curves are designed to visualize how a single factor affects the cooling intensity of a tree while the other variables are controlled to remain constant. Fig. 7 shows that Tree_Area, Tree_NDVI, and Tree_DEM are essentially positively correlated with the

cooling intensity, noting that the influence of Tree_NDVI on the cooling intensity is particularly prominent, which obviously strengthened as the value increases. It should be noted that although Tree_Area exhibits a positive correlation with cooling intensity, its cooling effect gradually weakens, which is of profound significance for interpreting the complex relationship between tree cover area and urban microclimate regulation. For Tree_DEM, it is positively correlated with cooling intensity when its value exceeds 100, both in winter and summer. Interestingly, TH_Mean is not simply linearly related to cooling intensity. Specifically, they are negatively correlated during summer ($\text{TH}_\text{Mean} < 12$) and winter ($\text{TH}_\text{Mean} < 14$), but the correlation turns significantly positive once this height threshold is exceeded.

4. Discussion

4.1. Global differences in the cooling effect of trees

To our knowledge, this study provides the first global insight into how 3D tree features contribution to the reducing of LST. Particularly noteworthy is that strong negative correlation is found between tree canopy height and LST. Although previous studies have explored the relationship, they mostly relied on a digital surface model to extract tree canopy heights, resulting in most previous studies being limited to a single or several cities. As a consequence, these studies failed to develop

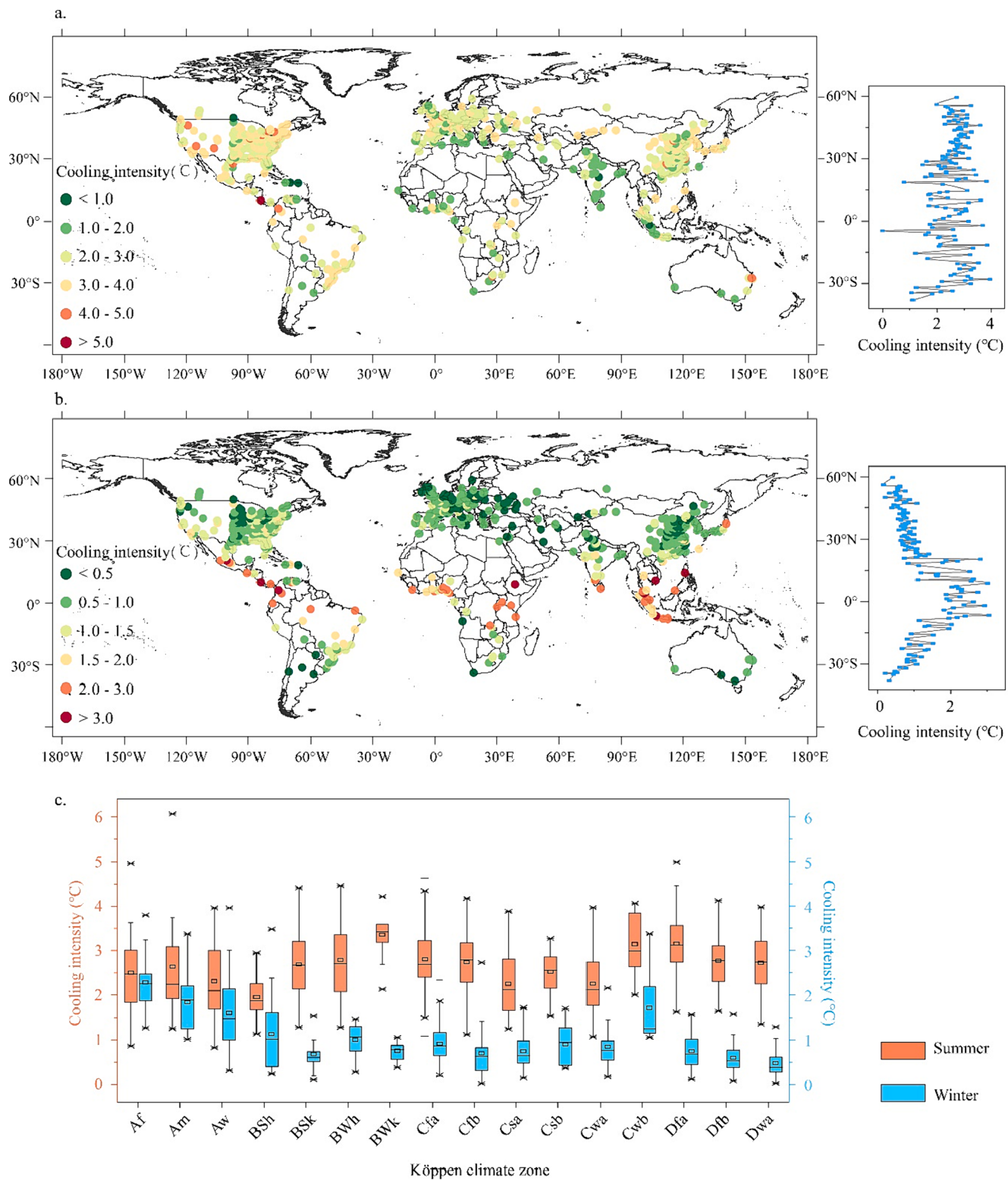


Fig. 5. Spatial distribution of tree cooling intensity (a and b represent cooling intensity in summer and winter, and c represents each climate zone).

a global understanding (Yu et al., 2018b). Correspondingly, this has also prevented previous studies from establishing a universally applicable law (Alexander, 2021; Wang et al., 2023b). In this study, we combined the global 10 m tree canopy height and LST, and found that the correlation between the two was higher than 0.80 in nearly 64 % of the total cities, further noting that nearly 95 % of the cities exceeded 0.50, which is similar to previous results for individual cities (Yu et al., 2018b).

Previous studies have less frequently explored the magnitude of the decrease in LST with increasing canopy height. Our findings indicate that for every 1 m increase in canopy height, the average LST drops by 0.16°C . This finding not only further emphasizes the important role of trees as green infrastructure in mitigating LST, but also provides solid quantitative support for future urban greening strategies and climate adaptation studies (Ronchi et al., 2020). Notably, the DEM acts as a key

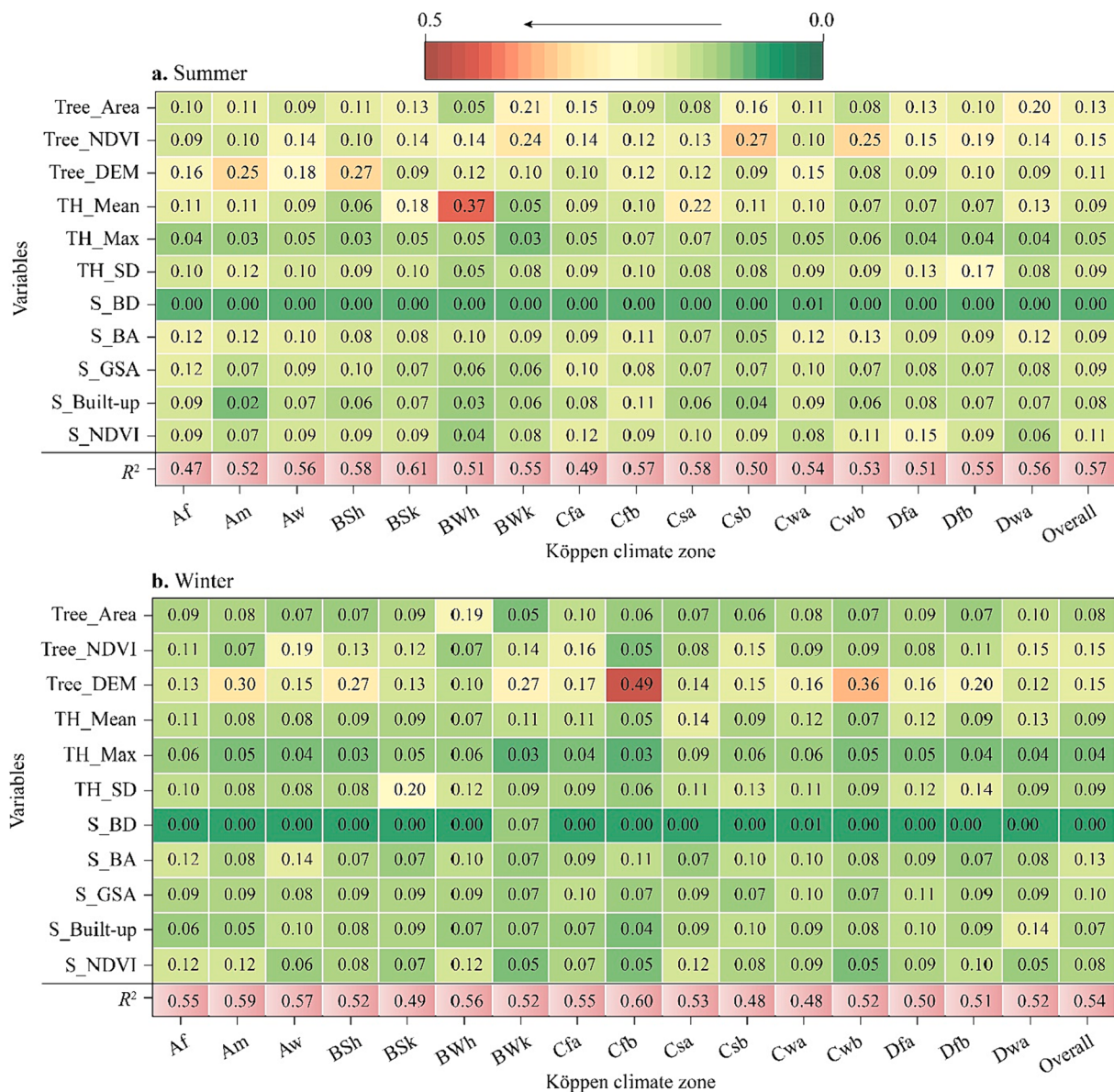


Fig. 6. Importance of factors affecting cooling intensity by climate zone (a and b represent summer and winter, respectively).

natural factor influencing LST. First, as altitude increases, the absorption of longwave radiation by atmosphere decreases, resulting in less heat stored in the atmosphere. The LST decreases due to the heat exchange process between the Earth's surface and atmosphere (Peng et al., 2020). Second, in areas with high altitudes and complex topography, there are fewer human activities, thus reducing the contribution of anthropogenic heat emissions to LST. To more accurately reveal the association between LST and canopy height, most scholars have used linear regression to eliminate the possible interference from elevation (Li et al., 2015; Cheng et al., 2022). Here, however, we focus on the relationship between LST and canopy height within each city boundary. Since elevation differences within each city are usually marginal, their interference with the final results is relatively limited. Overall, the role of canopy height in mitigating LST is likely to be related to its effects on urban landscape surface roughness, shading effects, air dispersion and wind speed (Gunawardena et al., 2017).

In the tropics (climate zone A), the variance in trees' cooling effects between winter and summer is relatively small, which is largely attributable to the stability of the climatic conditions in the region, such as small annual temperature differences, consistently high humidity, and

stable solar radiation. This stable climate reduces the effects of seasonal variations, allowing trees to perform photosynthesis and transpire similar. However, there were significant seasonal differences in tree-cooling effects in other climatic zones, with trees-cooling significantly more efficient in summer than in winter, which is consistent with previous studies (Wang et al., 2022). However, within the Dwa zone in winter, LST was higher in the tree-covered area compared to the surrounding built-up land. This phenomenon may be due to the wintertime inhibition of biophysical functions of trees, resulting in reduced or absent transpiration. In addition, trees promote snow retention, which isolates and stabilizes surface temperatures, this warming effect increases with warmer temperatures (Thompson et al., 2022). Interestingly, we found that the cooling effect of trees was relatively high in cities close to the equator in winter, we speculate that this is because trees therein are able to maintain their biological functions due to relatively stable heat and humidity conditions, thus leading to a relatively high cooling effect. However, at higher latitudes, where solar radiation and air temperatures are seasonal and relatively low, trees lose their leaves and transpiration is reduced, which in turn affects the cooling effect. Overall, climatic factors are undoubtedly one of the key

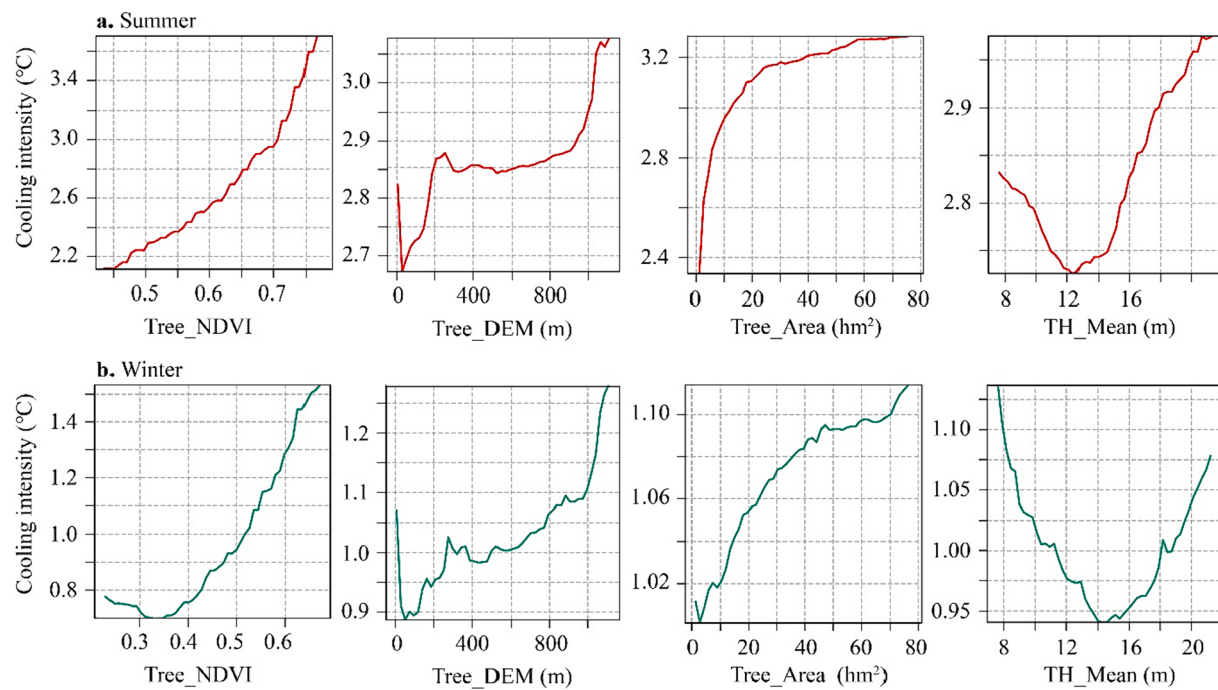


Fig. 7. Marginal effect curves of factors with tree cooling intensity.

variables influencing the cooling effect of trees.

4.2. Comparison of the importance of each factor for cooling intensity

Numerous studies have confirmed that the cooling intensity is not only governed by the tree's structural characteristics but is also affected by a combination of external factors such as geography, climate, and the surrounding environment (He et al., 2021). Our study demonstrated the significant influence of Tree_Area, Tree_NDVI, Tree_DEM, and TH_Mean in influencing the cooling intensity of trees, which fully emphasizes the centrality of the 3D tree features on cooling intensity. In addition, unlike previous studies that employed correlation and linear regression, we used the random forest algorithm to finely depict the marginal effect curves between each factor and tree-cooling intensity. Fig. 7 shows that Tree_Area, Tree_NDVI and Tree_DEM essentially maintain positive correlations with cooling intensity. Notably, trees' cooling intensity increased significantly with the increase of Tree_NDVI, recalling that NDVI metric represents the cover and health of vegetation (Feyisa et al., 2014). Although higher Tree Area values result in stronger cooling intensity, the magnitude of cooling gradually slows down, suggesting that urban heat mitigation through tree planting should not be pursued solely in terms of scale, but also in terms of its efficiency (Yu et al., 2020b). In addition, although a DEM is usually regarded as a key factor influencing LST, we found that the cooling intensity was only enhanced when Tree_DEM was higher than 100 m.

This study also enriched the effect of canopy height in terms of cooling intensity. Although canopy height showed a significant negative correlation with LST, its relationship with cooling intensity was more complex (Fig. 7). We found that TH_Mean showed a non-linear relationship with cooling intensity. The cooling intensity shifted towards a positive correlation after the canopy height reached the 12 m and 14 m thresholds in summer and winter, respectively, which may be due to the higher transpiration rates and shading effects of larger trees.

Our study also reveals that the surrounding building forms also exert a substantial role in influencing the cooling intensity of trees (Zhang et al., 2022). Although the biophysical properties of trees themselves play a dominant role in cooling, their surroundings, especially the neighboring built-up area, also have an important influence. It is worth

noting that we did not obtain globally consistent information on building morphology due to limitations on data acquisition and only considered the horizontal structural characteristics of buildings, ignoring the key variable of building height. A full understanding of the drivers of tree-cooling intensity will require consideration of the combined effects of more external factors in the neighborhood, including human activities.

4.3. Uncertainty and limitations

While this study offers a global perspective on the role of 3D urban tree features in reducing LST, it still has several limitations. First, it needs to be clear that our main focus is on LST, however, the LST here mainly records temperature information at the top of the tree, which means that it fails to adequately account for the complex thermal interaction phenomena under the tree canopy (Venter et al., 2021). It is worth noting that the SMW method is susceptible to total atmospheric water vapor content and suffers from an overestimation of LST, which subsequently affects the tree cooling effect (Ermida et al., 2020). Additionally, studies suggest that the effective anisotropy of thermal radiation induces variations in urban LST obtained by remote sensing (RS) when observed from different viewpoints (Wang et al., 2022; Duan et al., 2020). To address this issue, scholars have considered urban geometry, adjacency effects and material disturbances, and have combined techniques such as thermal cameras, high-resolution imagery GaoFen-5 (GF-5) and 3D rendering software to refine urban surface LST (Morrison et al., 2018; Morrison et al., 2021; Chen et al., 2021). These methodologies enhance the accuracy of urban LST, while these studies are constrained to local contexts due to the availability of high-resolution imagery and the complexity of model construction, among others. Moreover, there remain challenges in extending these approaches to a global scale. In addition, due to limitations in data acquisition, our analysis was confined to the cooling effect during the daytime and did not analyze the nighttime differences. Therefore, to investigate the tree-cooling effect and its differences between day and night, future studies should introduce more detailed data or fine-scale numerical models, or develop a new LST retrieval algorithm that integrates urban three-dimensional structural features (Chen et al., 2020).

Second, when extracting tree samples, it is difficult to avoid sample extraction errors due to the WorldCover 10 m data accuracy problem. In addition, we only considered the effect of canopy height on LST for a specific time period, which failed to reflect the dynamic characteristics of trees. Therefore, how to use remote sensing to track the temporal characteristics of trees and further explore their influence on tree-cooling effect represents a research direction where future work is needed. Finally, the cooling intensity is not only solely related to the disturbances inherent to the 3D tree pattern and surrounding environment but the species and health status of the tree also play an important role (Wetherley et al., 2018). For example, deciduous trees have a higher cooling effect, whereas trees infested with pests and diseases may be limited in their ability to transpire. Therefore, to understand the contribution of trees in reducing LST, subsequent studies should also examine these variables.

5. Conclusion

It is well known that trees are widely acknowledged as an efficient method to mitigate UHI effects. Although the role of 3D tree features in reducing LST has been investigated, there is still a relative lack of quantitative studies on this topic globally. In this study, we integrated Landsat 8 imagery, canopy height and building morphology datasets to comprehensively analyze the impacts of trees' 3D features on LST across various climatic zones around the world, and used the random forest method to reveal the significance of each contributing factor. Our findings show that LST in tree-covered areas is generally lower than in the surrounding built-up areas in summer, exhibiting an average decrease of 2.13 °C. However, the opposite phenomenon was observed in some cities in winter, especially in Dwa climate zone, where tree LST was instead higher by about 0.38 °C. In addition, tree canopy height showed a significant negative correlation with LST, and for every 1 m rise in height, LST decreased by approximately 0.16 °C. Interestingly, the tree-cooling effect was more significant in cities closer to the equatorial zone in winter, which was verified both in terms of LST differences and cooling intensity. Finally, although the factors affecting the cooling intensity differed across climate zones, the characteristics specific to the tree in question (Tree_Area, Tree_NDVI, Tree_DEM, and TH_Mean) were found to be important factors. Notably, the relationship between these factors and cooling intensity is not necessarily linear. For example, the relationship with cooling intensity becomes positive when the height of the tree exceeds 14 m. Overall, this study provides a strong data support for the three-dimensional characteristics of urban trees in reducing LST at a global scale.

CRediT authorship contribution statement

Tingting He: Conceptualization, Methodology, Data curation. **Yihua Hu:** Conceptualization, Funding acquisition. **Andong Guo:** Conceptualization, Writing – original draft, Funding acquisition. **Yuwei Chen:** Writing – review & editing. **Jun Yang:** Formal analysis. **Mengmeng Li:** Visualization. **Maoxin Zhang:** Validation.

Declaration of competing interest

The authors declare that they have no known competing financial interests or personal relationships that could have appeared to influence the work reported in this paper.

Acknowledgements

This research study was supported by National Natural Science Foundation of China (grant no. 42201307, 41771178), China Postdoctoral Science Foundation (2021M702789) and The Ministry of education of Humanities and Social Science project (22YJCZH042).

References

- Alexander, C., 2021. Influence of the proportion, height and proximity of vegetation and buildings on urban land surface temperature. *Int. J. Appl. Earth Obs. Geoinf.* 95, 102265 <https://doi.org/10.1016/j.jag.2020.102265>.
- Bartesaghi-Koc, C., Osmond, P., Peters, A., 2020. Quantifying the seasonal cooling capacity of 'green infrastructure types' (GITs): an approach to assess and mitigate surface urban heat island in Sydney, Australia. *Landscl. Urban Plan.* 203, 103893 <https://doi.org/10.1016/j.landurbplan.2020.103893>.
- Breiman, L., 2001. Random forests. *Mach. Learn.* 45, 5–32. <https://doi.org/10.1023/A:1010933404324>.
- Carlson, A.R., Helmers, D.P., Hawbaker, T.J., Mockrin, M.H., Radeloff, V.C., 2022. The wildland-urban interface in the United States based on 125 million building locations. *Ecol. Appl.* 32, e2597.
- Chang, Y., Xiao, J., Li, X., Weng, Q., 2023. Monitoring diurnal dynamics of surface urban heat island for urban agglomerations using ECOSTRESS land surface temperature observations. *Sust. Cities Soc.* 98, 104833 <https://doi.org/10.1016/j.scs.2023.104833>.
- Chen, J., Jin, S., Du, P., 2020. Roles of horizontal and vertical tree canopy structure in mitigating daytime and nighttime urban heat island effects. *Int. J. Appl. Earth Obs. Geoinf.* 89, 102060 <https://doi.org/10.1016/j.jag.2020.102060>.
- Chen, S., Ren, H., Ye, X., Dong, J., Zheng, Y., 2021. Geometry and adjacency effects in urban land surface temperature retrieval from high-spatial-resolution thermal infrared images. *Remote Sens. Environ.* 262, 112518 <https://doi.org/10.1016/j.rse.2021.112518>.
- Chen, B., Wu, S., Song, Y., Webster, C., Xu, B., Gong, P., 2022. Contrasting inequality in human exposure to greenspace between cities of Global North and Global South. *Nat. Commun.* 13 <https://doi.org/10.1038/s41467-022-32258-4>.
- Cheng, X., Peng, J., Dong, J., Liu, Y., Wang, Y., 2022. Non-linear effects of meteorological variables on cooling efficiency of African urban trees. *Environ. Int.* 169, 107489 <https://doi.org/10.1016/j.envint.2022.107489>.
- Du, S., Xiong, Z., Wang, Y., Guo, L., 2016. Quantifying the multilevel effects of landscape composition and configuration on land surface temperature. *Remote Sens. Environ.* 178, 84–92. <https://doi.org/10.1016/j.rse.2016.02.063>.
- Duan, S., Li, Z., Gao, C., Zhao, W., Wu, H., Qian, Y., Leng, P., Gao, M., 2020. Influence of adjacency effect on high-spatial-resolution thermal infrared imagery: implication for radiative transfer simulation and land surface temperature retrieval. *Remote Sens. Environ.* 245, 111852 <https://doi.org/10.1016/j.rse.2020.111852>.
- Ermida, S.L., Soares, P., Mantas, V., Götsche, F., Trigo, I.F., 2020. Google earth engine open-source code for land surface temperature estimation from the landsat series. *Remote Sens.* 12, 1471. <https://doi.org/10.3390/rs12091471>.
- Feyisa, G.L., Dons, K., Meilby, H., 2014. Efficiency of parks in mitigating urban heat island effect: an example from Addis Ababa. *Landscl. Urban Plan.* 123, 87–95. <https://doi.org/10.1016/j.landurbplan.2013.12.008>.
- Gage, E.A., Cooper, D.J., 2017. Urban forest structure and land cover composition effects on land surface temperature in a semi-arid suburban area. *Urban for. Urban Green.* 28, 28–35. <https://doi.org/10.1016/j.ufug.2017.10.003>.
- Gao, Y., Zhao, J., Han, L., 2023. Quantifying the nonlinear relationship between block morphology and the surrounding thermal environment using random forest method. *Sust. Cities Soc.* 91, 104443 <https://doi.org/10.1016/j.scs.2023.104443>.
- Grimm, N.B., Faeth, S.H., Golubiewski, N.E., Redman, C.L., Wu, J., Bai, X., Briggs, J.M., 2008. Global change and the ecology of cities. *Science* 319, 756–760. <https://doi.org/10.1126/science.1150195>.
- Gunawardena, K.R., Wells, M.J., Kershaw, T., 2017. Utilising green and bluespace to mitigate urban heat island intensity. *Sci. Total Environ.* 584–585, 1040–1055. <https://doi.org/10.1016/j.scitotenv.2017.01.158>.
- Guo, A., Yang, J., Sun, W., Xiao, X., Xia Cecilia, J., Jin, C., Li, X., 2020a. Impact of urban morphology and landscape characteristics on spatiotemporal heterogeneity of land surface temperature. *Sust. Cities Soc.* 63, 102443 <https://doi.org/10.1016/j.scs.2020.102443>.
- Guo, A., Yang, J., Xiao, X., Xia Cecilia, J., Jin, C., Li, X., 2020b. Influences of urban spatial form on urban heat island effects at the community level in China. *Sust. Cities Soc.* 53, 101972 <https://doi.org/10.1016/j.scs.2019.101972>.
- Guo, A., Yue, W., Yang, J., He, T., Zhang, M., Li, M., 2022. Divergent impact of urban 2D/3D morphology on thermal environment along urban gradients. *Urban Clim.* 45, 101278 <https://doi.org/10.1016/j.ulclim.2022.101278>.
- Guo, A., Yue, W., Yang, J., Xue, B., Xiao, W., Li, M., He, T., Zhang, M., Jin, X., Zhou, Q., 2023. Cropland abandonment in China: patterns, drivers, and implications for food security. *J. Clean Prod.* 418, 138154 <https://doi.org/10.1016/j.jclepro.2023.138154>.
- Han, L., Zhou, W., Li, W., 2015. City as a major source area of fine particulate (PM2.5) in China. *Environ. Pollut.* 206, 183–187. <https://doi.org/10.1016/j.envpol.2015.06.038>.
- He, C., Zhou, L., Yao, Y., Ma, W., Kinney, P.L., 2021. Cooling effect of urban trees and its spatiotemporal characteristics: a comparative study. *Build. Environ.* 204, 108103 <https://doi.org/10.1016/j.buildenv.2021.108103>.
- Howard, L., 1818. The climate of London: deduced from meteorological observations, made at different places in the neighbourhood of the metropolis. W. Phillips, George Yard, Lombard Street, sold also by J. and A. Arch.
- Hu, J., Zhou, Y., Yang, Y., Chen, G., Chen, W., Hejazi, M., 2023. Multi-city assessments of human exposure to extreme heat during heat waves in the United States. *Remote Sens. Environ.* 295, 113700 <https://doi.org/10.1016/j.rse.2023.113700>.
- Huang, X., Wang, Y., 2019. Investigating the effects of 3D urban morphology on the surface urban heat island effect in urban functional zones by using high-resolution remote sensing data: a case study of Wuhan, Central China. *ISPRS-J. Photogramm. Remote Sens.* 152, 119–131. <https://doi.org/10.1016/j.isprsjprs.2019.04.010>.

- Jungman, T., Cirach, M., Marando, F., Pereira Barboza, E., Khomenko, S., Masselot, P., Quijal-Zamorano, M., Mueller, N., Gasparini, A., Urquiza, J., Heris, M., Thondoo, M., Nieuwenhuijsen, M., 2023. Cooling cities through urban green infrastructure: a health impact assessment of European cities. *Lancet* 401, 577–589. [https://doi.org/10.1016/S0140-6736\(22\)02585-5](https://doi.org/10.1016/S0140-6736(22)02585-5).
- Lang, N., Jetz, W., Schindler, K., Wegner, J.D., 2022. A high-resolution canopy height model of the Earth. arXiv preprint arXiv:2204.08322. DOI: [10.48550/arXiv.2204.08322](https://doi.org/10.48550/arXiv.2204.08322).
- Leuzinger, S., Vogt, R., Körner, C., 2010. Tree surface temperature in an urban environment. *Agric. for. Meteorol.* 150, 56–62. <https://doi.org/10.1016/j.agrmet.2009.08.006>.
- Li, X., Gong, P., Zhou, Y., Wang, J., Bai, Y., Chen, B., Hu, T., Xiao, Y., Xu, B., Yang, J., Liu, X., Cai, W., Huang, H., Wu, T., Wang, X., Lin, P., Li, X., Chen, J., He, C., Li, X., Yu, L., Clinton, N., Zhu, Z., 2020. Mapping global urban boundaries from the global artificial impervious area (GAIA) data. *Environ. Res. Lett.* 15, 94044. <https://doi.org/10.1088/1748-9326/ab9be3>.
- Li, Y., Zhao, M., Motesharrei, S., Mu, Q., Kalnay, E., Li, S., 2015. Local cooling and warming effects of forests based on satellite observations. *Nat. Commun.* 6, 6603. <https://doi.org/10.1038/ncomms7603>.
- Liao, W., Guldmann, J., Hu, L., Cao, Q., Gan, D., Li, X., 2023. Linking urban park cool island effects to the landscape patterns inside and outside the park: a simultaneous equation modeling approach. *Landsc. Urban Plan.* 232, 104681. <https://doi.org/10.1016/j.landurbplan.2022.104681>.
- Liú, Z., Tang, H., Feng, L., Lyu, S., 2023. China Building Rooftop Area: the first multi-annual (2016–2021) and high-resolution (2.5 m) building rooftop area dataset in China derived with super-resolution segmentation from Sentinel-2 imagery. *Earth Syst. Sci. Data.* 15, 3547–3572. <https://doi.org/10.5194/essd-15-3547-2023>.
- Masoudi, M., Tan, P.Y., Liew, S.C., 2019. Multi-city comparison of the relationships between spatial pattern and cooling effect of urban green spaces in four major Asian cities. *Ecol. Indic.* 98, 200–213. <https://doi.org/10.1016/j.ecolind.2018.09.058>.
- Morrison, W., Kotthaus, S., Grimmond, C.S.B., Inagaki, A., Yin, T., Gastellu-Etchegorry, J., Kanda, M., Merchant, C.J., 2018. A novel method to obtain three-dimensional urban surface temperature from ground-based thermography. *Remote Sens. Environ.* 215, 268–283. <https://doi.org/10.1016/j.rse.2018.05.004>.
- Morrison, W., Kotthaus, S., Grimmond, S., 2021. Urban surface temperature observations from ground-based thermography: intra- and inter-facet variability. *Urban CLim.* 35, 100748. <https://doi.org/10.1016/j.uclim.2020.100748>.
- Napoli, M., Masetti, L., Brandani, G., Petrali, M., Orlandini, S., 2016. Modeling tree shade effect on urban ground surface temperature. *J. Environ. Qual.* 45, 146–156. <https://doi.org/10.2134/jeq2015.02.0097>.
- Nations, U., 2018. United Nations Department of Economic and Social Affairs. United Nations, New York.
- Parison, S., Chaumont, M., Kounkou-Arnaud, R., Long, F., Bernik, A., Da Silva, M., Hendel, M., 2023. The effects of greening a parking lot as a heat mitigation strategy on outdoor thermal stress using fixed and mobile measurements: case-study project “tertiary forest”. *Sust. Cities Soc.* 98, 104818. <https://doi.org/10.1016/j.scs.2023.104818>.
- Park, M., Hagishima, A., Tanimoto, J., Narita, K., 2012. Effect of urban vegetation on outdoor thermal environment: field measurement at a scale model site. *Build. Environ.* 56, 38–46. <https://doi.org/10.1016/j.buildenv.2012.02.015>.
- Patz, J.A., Campbell-Lendrum, D., Holloway, T., Foley, J.A., 2005. Impact of regional climate change on human health. *Nature* 438, 310–317. <https://doi.org/10.1038/nature04188>.
- Peel, M.C., Finlayson, B.L., McMahon, T.A., 2007. Updated world map of the Köppen-Geiger climate classification. *Hydrol. Earth Syst. Sci.* 11, 1633–1644. <https://doi.org/10.5194/hess-11-1633-2007>.
- Peng, J., Dan, Y., Qiao, R., Liu, Y., Dong, J., Wu, J., 2021. How to quantify the cooling effect of urban parks? Linking maximum and accumulation perspectives. *Remote Sens. Environ.* 252, 112135. <https://doi.org/10.1016/j.rse.2020.112135>.
- Peng, X., Wu, W., Zheng, Y., Sun, J., Hu, T., Wang, P., 2020. Correlation analysis of land surface temperature and topographic elements in Hangzhou, China. *Sci Rep.* 10 (1), 10451. <https://doi.org/10.1038/s41598-020-67423-6>.
- Peng, W., Wu, Z., Duan, J., Gao, W., Wang, R., Fan, Z., Liu, N., 2023. Identifying and quantizing the non-linear correlates of city shrinkage in Japan. *Cities* 137, 104292. <https://doi.org/10.1016/j.cities.2023.104292>.
- Rahman, M.A., Stratopoulos, L.M.F., Moser-Reischl, A., Zöllch, T., Häberle, K., Rötzer, T., Pretzsch, H., Pauleit, S., 2020. Traits of trees for cooling urban heat islands: a meta-analysis. *Build. Environ.* 170, 106606. <https://doi.org/10.1016/j.buildenv.2019.106606>.
- Ronchi, S., Arcidiacono, A., Pogliani, L., 2020. Integrating green infrastructure into spatial planning regulations to improve the performance of urban ecosystems. Insights from an Italian case study. *Sust. Cities Soc.* 53, 101907. <https://doi.org/10.1016/j.scs.2019.101907>.
- Speak, A., Montagnani, L., Wellstein, C., Zerbe, S., 2020. The influence of tree traits on urban ground surface shade cooling. *Landsc. Urban Plan.* 197, 103748. <https://doi.org/10.1016/j.landurbplan.2020.103748>.
- Tan, X., Sun, X., Huang, C., Yuan, Y., Hou, D., 2021. Comparison of cooling effect between green space and water body. *Sust. Cities Soc.* 67, 102711. <https://doi.org/10.1016/j.scs.2021.102711>.
- Thompson, K.L., Pauli, J.N., Erker, T., Kucharik, C.J., Schatz, J., Townsend, P.A., Zuckerberg, B., 2022. Urban greenspaces promote warmer soil surface temperatures in a snow-covered city. *Landsc. Urban Plan.* 227, 104537. <https://doi.org/10.1016/j.landurbplan.2022.104537>.
- Venter, Z.S., Chakraborty, T., Lee, X., 2021. Crowdsourced air temperatures contrast satellite measures of the urban heat island and its mechanisms. *Sci. Adv.* 7, b9569. <https://doi.org/10.1126/sciadv.abb9569>.
- Voogt, J.A., Oke, T.R., 2003. Thermal remote sensing of urban climates. *Remote Sens. Environ.* 86, 370–384. [https://doi.org/10.1016/S0034-4257\(03\)00079-8](https://doi.org/10.1016/S0034-4257(03)00079-8).
- Wang, Z., Liang, L., Sun, Z., Wang, X., 2019b. Spatiotemporal differentiation and the factors influencing urbanization and ecological environment synergistic effects within the Beijing-Tianjin-Hebei urban agglomeration. *J. Environ. Manage.* 243, 227–239. <https://doi.org/10.1016/j.jenvman.2019.04.088>.
- Wang, X., Rahman, M.A., Mokroš, M., Rötzer, T., Pattnaik, N., Pang, Y., Zhang, Y., Da, L., Song, K., 2023b. The influence of vertical canopy structure on the cooling and humidifying urban microclimate during hot summer days. *Landsc. Urban Plan.* 238, 104841. <https://doi.org/10.1016/j.landurbplan.2023.104841>.
- Wang, C., Wang, Z., Wang, C., Myint, S.W., 2019a. Environmental cooling provided by urban trees under extreme heat and cold waves in U.S. cities. *Remote Sens. Environ.* 227, 28–43. <https://doi.org/10.1016/j.rse.2019.03.024>.
- Wang, C., Ren, Z., Dong, Y., Zhang, P., Guo, Y., Wang, W., Bao, G., 2022. Efficient cooling of cities at global scale using urban green space to mitigate urban heat island effects in different climatic regions. *Urban for. Urban Green.* 74, 127635. <https://doi.org/10.1016/j.ufug.2022.127635>.
- Wang, J., Zhou, W., Jiao, M., Zheng, Z., Ren, T., Zhang, Q., 2020. Significant effects of ecological context on urban trees' cooling efficiency. *ISPRS-J. Photogramm. Remote Sens.* 159, 78–89. <https://doi.org/10.1016/j.isprsjprs.2019.11.001>.
- Wang, J., Zhou, W., Zheng, Z., Jiao, M., Qian, Y., 2023a. Interactions among spatial configuration aspects of urban tree canopy significantly affect its cooling effects. *Sci. Total Environ.* 864, 160929. <https://doi.org/10.1016/j.scitotenv.2022.160929>.
- Wetherley, E.B., McFadden, J.P., Roberts, D.A., 2018. Megacity-scale analysis of urban vegetation temperatures. *Remote Sens. Environ.* 213, 18–33. <https://doi.org/10.1016/j.rse.2018.04.051>.
- Winbourne, J.B., Jones, T.S., Garvey, S.M., Harrison, J.L., Wang, L., Li, D., Templer, P.H., Hutyra, L.R., 2020. Tree transpiration and urban temperatures: current understanding, implications, and future research directions. *Bioscience* 70, 576–588. <https://doi.org/10.1093/biosci/bia055>.
- Yang, Q., Huang, X., Yang, J., Liu, Y., 2021. The relationship between land surface temperature and artificial impervious surface fraction in 682 global cities: spatiotemporal variations and drivers. *Environ. Res. Lett.* 16, 24032. <https://doi.org/10.1088/1748-9326/abdaed>.
- Yang, Q., Huang, X., Tong, X., Xiao, C., Yang, J., Liu, Y., Cao, Y., 2022. Global assessment of urban trees' cooling efficiency based on satellite observations. *Environ. Res. Lett.* 17, 34029. <https://doi.org/10.1088/1748-9326/ac4c1c>.
- Yin, Y., He, L., Wennberg, P.O., Frankenberg, C., 2023. Unequal exposure to heatwaves in Los Angeles: impact of uneven green spaces. *Sci. Adv.* 9, e8501.
- Yu, Q., Acheampong, M., Pu, R., Landry, S.M., Ji, W., Dahigamuwa, T., 2018a. Assessing effects of urban vegetation height on land surface temperature in the City of Tampa, Florida, USA. *Int. J. Appl. Earth Obs. Geoinf.* 73, 712–720. <https://doi.org/10.1016/j.jag.2018.08.016>.
- Yu, Q., Ji, W., Pu, R., Landry, S., Acheampong, M., O Neil-Dunne, J., Ren, Z., Tanim, S.H., 2020a. A preliminary exploration of the cooling effect of tree shade in urban landscapes. *Int. J. Appl. Earth Obs. Geoinf.* 92, 102161. <https://doi.org/10.1016/j.jag.2020.102161>.
- Yu, Z., Xu, S., Zhang, Y., Jørgensen, G., Vejre, H., 2018b. Strong contributions of local background climate to the cooling effect of urban green vegetation. *Sci. Rep.* 8, 6798. <https://doi.org/10.1038/s41598-018-25296-w>.
- Yu, Z., Yang, G., Zuo, S., Jørgensen, G., Koga, M., Vejre, H., 2020b. Critical review on the cooling effect of urban blue-green space: a threshold-size perspective. *Urban Urban Green.* 49, 126630. <https://doi.org/10.1016/j.ufug.2020.126630>.
- Zanaga, D., Van De Kerchove, R., De Keersmaecker, W., Souverijns, N., Brockmann, C., Quast, R., Wevers, J., Grosu, A., Paccini, A., Vergnaud, S., Cartus, O., Santoro, M., Fritz, S., Georgieva, I., Lesiv, M., Carter, S., Herold, M., Li, L., Tsendbazar, N., Ramoino, F., Arino, O., 2021. ESA WorldCover 10 m 2020 v100. DOI: [10.5281/zanaga.5571936](https://doi.org/10.5281/zanaga.5571936).
- Zhang, Q., Zhou, D., Xu, D., Rogora, A., 2022. Correlation between cooling effect of green space and surrounding urban spatial form: evidence from 36 urban green spaces. *Build. Environ.* 222, 109375. <https://doi.org/10.1016/j.buldev.2022.109375>.
- Zhao, J., Zhao, X., Wu, D., Meili, N., Faticchi, S., 2023. Satellite-based evidence highlights a considerable increase of urban tree cooling benefits from 2000 to 2015. *Glob. Change Biol.* 29, 3085–3097. <https://doi.org/10.1111/gcb.16667>.
- Zhou, W., Wang, J., Cadena, M.L., 2017. Effects of the spatial configuration of trees on urban heat mitigation: a comparative study. *Remote Sens. Environ.* 195, 1–12. <https://doi.org/10.1016/j.rse.2017.03.043>.